state was proposed as a possible mechanism in Lineberger's earlier study (*11*), our experiments provide conclusive spectroscopic evidence that this occurs.

REFERENCES AND NOTES

1. A. H. Zewail, *J. Phys. Chem.* **100**, 12701 (1996).
2. P. L. Houston, *ibid.*, p. 12757.
3. M. H. Head-Gordon, *ibid.*, p. 13213.
4. G. C. Schatz, *ibid.*, p. 12839.
5. A. W. Castleman and K. H. Bowen, *ibid.*, p. 12911.
6. B. J. Greenblatt, M. T. Zanni, D. M. Neumark, *Chem. Phys. Lett.* **258**, 523 (1996).
7. D. R. Cyr and C. C. Hayden, *J. Chem. Phys.* **104**, 771 (1996).
8. P. Ludowise, M. Blackwell, Y. Chen, *Chem. Phys. Lett.* **258**, 530 (1996).
9. A. Assion, M. Geisler, J. Helbing, V. Seyfried, T. Baumert, *Phys. Rev. A* **54**, R4605 (1996).
10. J. M. Papanikolas *et al.*, *J. Chem. Phys.* **99**, 8733 (1993).
11. V. Vorsa, P. J. Campagnola, S. Nandi, M. Larsson, W. C. Lineberger, *ibid.* **105**, 2298 (1996).
12. V. Vorsa, S. Nandi, P. J. Campagnola, M. Larsson, W. C. Lineberger, *ibid.* **106**, 1402 (1997).
13. Q. Liu, J.-K. Wang, A. H. Zewail, *Nature* **364**, 427 (1993).
14. E. C. M. Chen and W. E. Wentworth, *J. Phys. Chem.* **89**, 4099 (1985).
15. M. T. Zanni, T. Taylor, B. J. Greenblatt, B. Soep, D. M. Neumark, in preparation.
16. D. R. T. Appadoo *et al.*, *J. Chem. Phys.* **104**, 903 (1996).
17. I. Yourshaw, Y. X. Zhao, D. M. Neumark, *ibid.* **105**, 351 (1996).
18. L. Perera and F. G. Amar, *ibid.* **90**, 7354 (1989).
19. J. Faeder, N. Delaney, P. E. Maslen, R. Parson, *Chem. Phys. Lett.* **270**, 196 (1997).
20. J. Faeder and R. Parson, in preparation.
21. V. S. Batista and D. F. Coker, *J. Chem. Phys.* **106**, 7102 (1997).
22. P. E. Maslen, J. Faeder, R. Parson, *Chem. Phys. Lett.* **263**, 63 (1997).
23. Supported by NSF under grant number CHE-9404735 and the Defense University Research Instrumentation Program under grant number F49620-95-1-0078. We thank J. Faeder, P. Maslen, V. Batista, and R. Parson for helpful discussions and for providing access to unpublished results. We are grateful to R. J. Le Roy for a copy of *RKR1: A Computer Program for Implementing the First-Order RKR Method for Determining Diatom Potential Energy Curves from Spectroscopic Constants*.

19 February 1997; accepted 12 May 1997

Infrared Spectrum of a Molecular Ice Cube: The S_4 and D_{2d} Water Octamers in Benzene-(Water)$_8$

Christopher J. Gruenloh, Joel R. Carney, Caleb A. Arrington,
Timothy S. Zwier,* Sharon Y. Fredericks, Kenneth D. Jordan*

Resonant two-photon ionization, ultraviolet hole-burning, and resonant ion-dip infrared (RIDIR) spectroscopy were used to assign and characterize the hydrogen-bonding topology of two conformers of the benzene-(water)$_8$ cluster. In both clusters, the eight water molecules form a hydrogen-bonded cube to which benzene is surface-attached. Comparison of the RIDIR spectra with density functional theory calculations is used to assign the two (water)$_8$ structures in benzene-(water)$_8$ as cubic octamers of D_{2d} and S_4 symmetry, which differ in the configuration of the hydrogen bonds within the cube. OH stretch vibrational fundamentals near 3550 wave numbers provide unique spectral signatures for these "molecular ice cubes."

The gas-phase water octamer (W_8) holds a unique position among water clusters. From a structural viewpoint, both ab initio (*1, 2*) and model-potential (*1, 3–5*) calculations have predicted that the lowest energy structure for the octamer is nominally cubic, with the eight tricoordinated water molecules taking up positions at the corners of the cube. Such H-bond–deficient water molecules are known to be present at the surface of ice (*6*) and liquid water (*7*), and the cubic W_8 cluster enables the study of tricoordinate water molecules free from interference from the tetracoordinated molecules that dominate the bulk condensed phases. Furthermore, the cubic water clusters are prototypical building blocks for larger fused-cubic or cuboid structures, which have been proposed to play an important role in larger (water)$_n$ clusters (*4, 5*).

The water octamer can form six cubic structures, which differ in the orientations of the H bonds in the cube. Of these, the D_{2d} and S_4 symmetry structures have been calculated to be ~2 kcal/mol more strongly bound than the other four (*4*). The D_{2d} and S_4 structures each contain 12 H bonds: four in each of two cyclic tetramer subunits, and four bridging the two tetramers. The two structures are distinguished in having the H bonds within the tetramers oriented in the opposite (D_{2d}) or same (S_4) directions.

One of the most powerful spectroscopic probes of H-bonding networks is the OH stretch region of the infrared (IR) (*8*). The vibrational frequency and IR intensity of the OH stretch fundamentals are sensitive functions of the number, type, and strength of H bonds in which each OH group participates. Recent IR spectroscopic studies of small water (W_n) (*9*) and benzene-(water)$_n$ (BW_n) clusters (*10–13*) have provided insight into the structural and dynamic consequences of networks of H bonds. Here we report the corresponding OH-stretch IR spectral signatures for the D_{2d} and S_4 water octamers complexed to a single benzene molecule. The benzene molecule provides a means for both size and conformational selection of the clusters and weakly perturbs the W_8 cluster so that intensity is induced in many of the IR transitions that would otherwise be symmetry forbidden.

Ultraviolet spectra of the BW_n clusters were recorded with the use of resonant two-photon ionization (R2PI)–time-of-flight mass spectroscopy (*13–15*), monitoring the BW_6^+ and BW_7^+ mass channels (Fig. 1, curves A and B, respectively) in the origin region of the $S_1 \leftarrow S_0$ transition from the ground to the first excited singlet state of benzene. This transition from the lowest vibrational level of the S_0 state to the lowest vibrational level of the S_1 state is electric-dipole forbidden (*16*); however, in the BW_8 clusters, the presence of the water molecules lowers the symmetry, thereby inducing some intensity in the transition.

The assignment of a spectral transition to a given neutral cluster size must take into account the fragmentation of the cluster that can follow photo-ionization. Previous work (*13, 14*) has shown that in one-color R2PI experiments, BW_n clusters with $n = 1$ to 6 fragment after photo-ionization by loss of a single water molecule ($BW_n + 2h\nu \rightarrow BW_{n-1}^+ + W$), but larger clusters fragment to give both BW_{n-1}^+ and BW_{n-2}^+ (*14*). Thus, most of the structure in the BW_6^+ mass channel (Fig. 1, curve A) is from BW_7 and BW_8, whereas that in the BW_7^+ channel (Fig. 1, curve B) arises from BW_8 and BW_9. The set of four transitions marked in Fig. 1 appears primarily in the BW_7^+ mass channel but also in BW_6^+ and is therefore assigned to the BW_8 neutral cluster.

To determine whether more than one species contributes to the set of ultraviolet (UV) transitions assigned to BW_8, UV-UV hole-burning spectroscopy was performed (*17*). In these spectra, a high-power UV laser pulse was used to remove a significant fraction of the ground-state population of a given species. A second UV laser was then tuned through the spectrum while the difference in ion signal with and without the hole-burning laser present was recorded.

C. J. Gruenloh, J. R. Carney, C. A. Arrington, T. S. Zwier, Department of Chemistry, Purdue University, West Lafayette, IN 47907-1393, USA.
S. Y. Fredericks and K. D. Jordan, Department of Chemistry, University of Pittsburgh, Pittsburgh, PA 15260, USA.

*To whom correspondence should be addressed. E-mail: zwier@chem.purdue.edu, jordan@cpwsca.psc.edu

Any transition that shares its initial level with that used in the hole-burning step appeared as a positive signal in the hole-burning spectrum. The R2PI spectrum in the region of the more intense 6_0^1 transition of benzene (that is, from vibrational quantum number $v = 0$ in S_0 to $v = 1$ in ν_6 in S_1) divides into two parts under hole-burning (Fig. 2, curves A and B), indicating that two structural isomers of BW_8 are responsible for the R2PI spectrum (Fig. 2, curve C). The degeneracy of the 6^1 level of benzene is split by the interaction with W_8 to form a doublet.

The UV spectra of the two structural isomers of BW_8 hold several clues to the nature of the BW_8 species. On the one hand, the spectra of BW_8(I) and BW_8(II) are nearly identical, suggesting that the two structural isomers are close analogs of one another. First, the UV transitions of the isomers are separated by only 4.2 cm^{-1}. Second, the spectra of I and II have similar 6_0^1 splittings (2.0 and 2.3 cm^{-1}, respectively), indicating that the W_n species induce similar asymmetry in the benzene molecule. Third, the spectra of both species exhibit a second, weak transition 7 cm^{-1} above the main band (Fig. 2), which is probably due to combination bands involving a low-frequency intermolecular vibration in the cluster.

On the other hand, the R2PI spectra of the two BW_8 structural isomers show significant differences from the spectra of BW_6 and BW_7, suggesting that the structure of BW_8 differs significantly from those two structures. First, the transitions due to BW_8 are shifted at least 40 cm^{-1} from those due to BW_6 (+110 cm^{-1}) and BW_7 (+139 cm^{-1}). The frequency shift from BW_7 to BW_8 is larger than any other one-water shift observed in the smaller BW_n clusters (*10*). Second, the extent of fragmentation after the photo-ionization of BW_8 is significantly less than that in BW_7. Such a reduction in fragmentation indicates that the BW_8 structural isomers are significantly more stable than BW_7.

Infrared spectra of the two BW_8 structural isomers were recorded by resonant ion-dip IR (RIDIR) spectroscopy (*11, 13*). We selected a single size and conformation of cluster for study in the IR by monitoring its ion signal with the UV-laser wavelength set on the cluster's transition in the R2PI spectrum. The IR spectrum was then recorded as a depletion of the BW_6^+ ion signal induced by an IR laser pulse whenever an IR transition occurred out of the same ground-state level as that monitored in R2PI.

The RIDIR spectra of BW_8(I) and BW_8(II) in the OH stretch region (Fig. 3, A and B, respectively) are strikingly similar to one another and comparatively simple, belying similar, high-symmetry W_8 structures. The OH stretch absorptions (Table 1) can be assigned to one of four hydrogen-bonding types. (i) The transitions due to the free OH groups (F) appear as a single, unresolved absorption at 3713.5 cm^{-1}. (ii) π H-bonded OH absorptions (π) occur near 3650 cm^{-1}, associated with the weak bond formed by the interaction of one of the dangling OH groups on the water octamer with the aromatic π cloud of benzene. (iii) The absorptions near 3550 cm^{-1} are assigned to double-donor (D) water molecules. It is here that the most significant differences between the spectra of the two BW_8 isomers appear: BW_8(I) has two re-

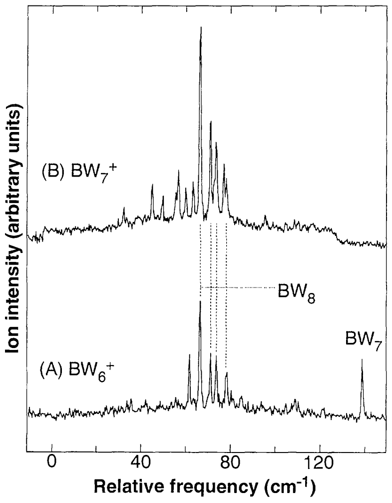

Fig. 1. One-color resonant two-photon ionization spectra of BW_n clusters near the origin of the $S_1 \leftarrow S_0$ transition of benzene, monitoring the BW_n^+ ions with (curve A) $n = 6$ and (curve B) $n = 7$. The zero of the frequency scale is taken to be the forbidden origin of the $S_1 \leftarrow S_0$ transition for the benzene monomer (38,086 cm^{-1}). The assignment of transitions to BW_7 and BW_8 are given in the spectrum. Fragmentation of the BW_n clusters after photo-ionization causes efficient loss of one or two water molecules. The BW_7 cluster then appears in the BW_5^+ and BW_6^+ mass channels, and BW_8 appears in the BW_6^+ and BW_7^+ mass channels. The unlabeled transitions are assigned to larger B_mW_n clusters.

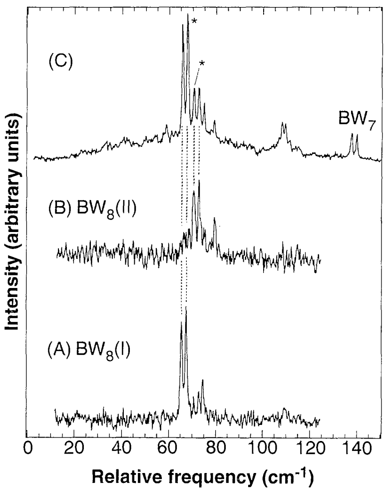

Fig. 2. (Curves A and B) Ultraviolet hole-burning spectra of the transitions assigned to BW_8 in the 6_0^1 region, which lies 521 cm^{-1} above the $S_1 \leftarrow S_0$ origin. The hole-burning laser is tuned to the transitions (A) 67.6 cm^{-1} and (B) 70.3 cm^{-1} above the 6_0^1 transition of free benzene, marked by asterisks in curve C. (Curve C) The one-color R2PI spectrum for comparison. The BW_6^+ mass channel is monitored because the BW_8 transitions are most cleanly observed in this mass channel. The R2PI spectrum in the 6_0^1 region differs from that at the origin (Fig. 1) in that (i) each transition at the origin is a doublet at 6_0^1 because of the near degeneracy of the 6^1 level, (ii) the relative intensities of transitions are affected by the different efficiencies of fragmentation with changing cluster size, and (iii) the relative intensities of the origin transitions relative to those at 6_0^1 vary depending on the symmetry-breaking effect of the water cluster on benzene.

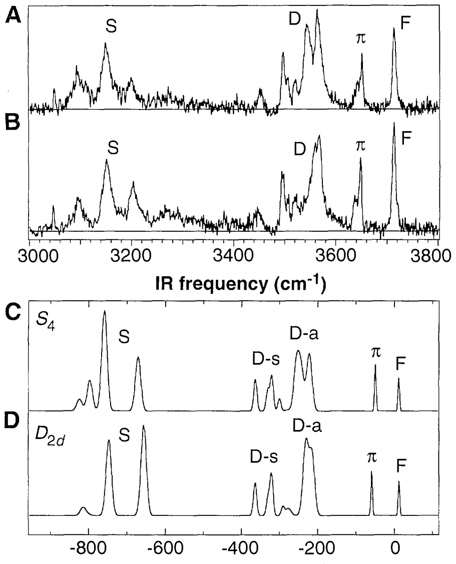

Fig. 3. (**A** and **B**) Resonant ion-dip IR spectra of the transitions (A) 67.6 cm^{-1} and (B) 70.3 cm^{-1} above the 6_0^1 transition of free benzene, corresponding to BW_8(I) and BW_8(II) from Fig. 2, curves A and B, respectively. The OH stretch fundamentals assigned to free OH (F), π H-bonded OH (π), symmetric stretch (D-s) and antisymmetric stretch (D-a) double-donor OH, and single-donor OH groups (S) are indicated. The sharp transitions at 3048 cm^{-1} and 3101 cm^{-1} are C-H stretch fundamentals of the benzene molecule in the cluster. (**C** and **D**) OH stretch vibrational frequency shifts and IR intensities calculated for the OH stretch normal modes of $BW_8(S_4)$ and $BW_8(D_{2d})$ using density functional theory. The zero of the frequency-shift scale is taken to be the average of the calculated frequencies of the symmetric and antisymmetric stretch modes of the water monomer. The calculated transitions are given Gaussian widths corresponding to the experimental widths from (A) and (B).

solved double-donor bands that dominate the double-donor transitions, whereas BW_8(II) has a single band dominating this region. (iv) The single-donor OH absorptions (S) appear below 3300 cm^{-1}.

As an aid in assigning and analyzing the RIDIR spectra, density functional theory (DFT) calculations of the structures, binding energies, harmonic vibrational frequencies, and IR intensities have been carried out on the S_4 and D_{2d} W_8 isomers both in the presence and absence of benzene. The DFT calculations use the Becke3LYP functional (*18*) with 6-31+G[d,p] (*19*) and 6-31G(d) (*20*) basis sets on the water and benzene molecules, respectively (*21*, *22*). The geometries were optimized using analytical gradients, and the frequencies were obtained using analytical second derivatives. The calculations were carried out using the Gaussian 94 program (*23*).

The binding energies calculated for the optimized $W_8(D_{2d})$ and $W_8(S_4)$ clusters (Fig. 4, A and B) are nearly identical. In the absence of vibrational zero-point energy (ZPE) corrections, the D_{2d} structure is predicted to be 0.06 kcal/mol more strongly bound than S_4, but this energy ordering is reversed (with S_4 lower by 0.11 kcal/mol) when ZPE is included. In these free D_{2d} and S_4 water octamers, the oxygen atoms do not form a perfect cube, but distort to accommodate four shorter AAD→ADD hydrogen bonds (2.64 Å) and eight longer ADD→AAD (2.83 Å) hydrogen bonds (AAD and ADD refer to double-acceptor–single-donor and single-acceptor–double-donor water molecules, respectively).

The DFT calculations on the analogous BW_8 clusters lead to structures in which benzene is attached to the surface of the W_8 structures by a π H bond to one of the free OH groups on the cluster (Fig. 4, C and D). The presence of the benzene molecule causes only small distortions in the S_4 and D_{2d} W_8 clusters (Table 2). Moreover, the binding energies of the benzene molecule to the two W_8 isomers are within 0.02 kcal/mol of one another.

The agreement of the calculated spectra (Fig. 3, C and D) with experiment (Fig. 3, A and B) is sufficiently good to confirm the proposed assignment of the BW_8 isomers responsible for the experimental spectra (*24*). In the bare W_8 clusters, the strongest double-donor IR fundamentals are nominally antisymmetric stretch in character (D-a), delocalized over the four double-donor water molecules in the cube. In the D_{2d} isomer, a single band ascribed to a degenerate pair of vibrations with frequency shift of −222 cm^{-1} carries all the antisymmetric double-donor (D-a) intensity. In contrast, in the S_4 isomer there are two double-donor bands separated by 20 cm^{-1} that are predicted to carry the D-a intensity (one nondegenerate and one doubly degenerate). This difference is maintained in the presence of benzene, which splits the allowed degenerate pair of vibrations in both the D_{2d} and S_4 isomers, by 10 to 13 cm^{-1},

Table 1. Experimental vibrational frequencies, widths, and relative integrated intensities for the two structural isomers of benzene-(water)$_8$. The widths are full widths at half-maximum in wave numbers. The intensities are approximate power-normalized, integrated intensities for each type of OH stretch, scaled to a value of 3.00 for the free OH, because three free OH groups are present in the BW_8 isomers. They have not been corrected for the effects of partial saturation of the transitions. The double-donor and single-donor OH stretch transitions gain intensity through their H bonds with other water molecules.

Vibrational type	No. of OH groups	II [$BW_8(D_{2d})$]			I [$BW_8(S_4)$]		
		Freq.	Width	Int.	Freq.	Width	Int.
Free OH	3	3713.5	7	3	3713.5	7	3
π H-bonded OH	1	3649	6	4	3650	6	4
		3637	8		3642	8	
Double-donor OH stretches	8						
Antisymmetric		3568	25	20	3563	20	29
		3543	20				
Symmetric		3523	13	12	3520	9	12
		3508	~8		3506	~8	
		3497	9		3496	8	
		3446	12		3454	10	
Single-donor OH stretches	4	3203	19	18	3198	~20	16
		3151	21		3148	20	
		3097	16		3092	20	
CH stretch region of benzene		3046.5	4	~0.6	3048	4	~0.5

Table 2. Key structural data calculated for the S_4 and D_{2d} isomers of W_8 and BW_8 using density functional theory. R is the O-O separation, and r is the O-H bond length, in angstroms (for atom numbering, see Fig. 4). Rotational constants are in gigahertz, and dipole moments are in debye.

Parameter	$W_8(S_4)$	$BW_8(S_4)$	$W_8(D_{2d})$	$BW_8(D_{2d})$
$R(O_1\text{-}O_2)$	2.641	2.671	2.645	2.674
$R(O_1\text{-}O_4)$	2.833	2.800	2.827	2.791
$R(O_1\text{-}O_5)$	2.828	2.791	2.827	2.791
$r(O_1\text{-}H_2)$	1.008	1.002	1.008	1.002
$r(O_4\text{-}H_3)$	0.983	0.986	0.983	0.986
$r(O_5\text{-}H_4)$	0.983	0.986	0.983	0.986
$r(O_1\text{-}H_1)$	0.967	0.971	0.967	0.971
$r(X\text{-}H_1)$*	2.503	2.517		
$r(X\text{-}O_1)$*	3.455	3.453		
Dipole moments	0	1.26	0	1.23
Rotational constants	0.92437	0.68811	0.92529	0.69246
	0.89338	0.21141	0.92529	0.21637
	0.89338	0.21501	0.86387	0.21346

*X is the center of mass of benzene.

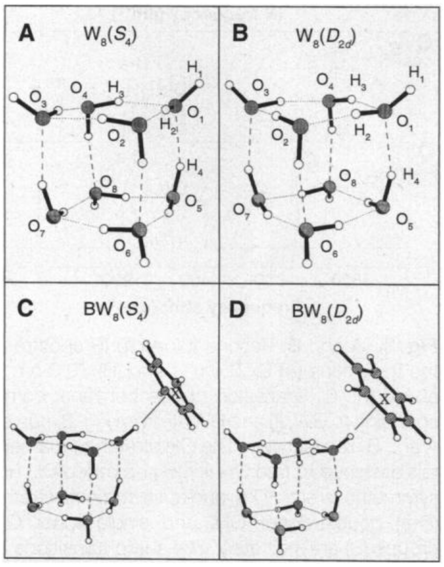

Fig. 4. Calculated structures for the (**A**) S_4 and (**B**) D_{2d} symmetry cubic water octamers and the corresponding structures calculated for (**C**) $BW_8(S_4)$ and (**D**) $BW_8(D_{2d})$. The two structures differ in the orientation of the 12 H bonds in the cube. The top and bottom faces can be viewed as cyclic tetramer subunits that have their H bonds either in the same (S_4) or opposite (D_{2d}) directions. The presence of benzene causes a local distortion of the cubic W_8 clusters, with the distortion being greater near the site of attachment.

an amount insufficient to be resolved in the experimental spectra given the inherent width of the transitions (20 cm^{-1}). The comparison with the experimental spectra (Fig. 3, A and B) leads to an assignment of BW_8(I) as BW_8 (cubic S_4) and BW_8(II) as BW_8(cubic D_{2d}). Weaker transitions, due to the symmetric-stretch double-donor transitions, are observed between 3450 and 3520 cm^{-1}, also consistent with the predictions of the calculations.

The change induced by benzene in the single-donor region is larger than that in the double-donor transitions. In the absence of benzene, the single-donor normal modes are delocalized over all four single-donor OH groups in the cube. By symmetry, all of the single-donor IR intensity is concentrated in a single transition in $W_8(D_{2d})$ and in a doubly degenerate set of transitions in $W_8(S_4)$. Because the binding of benzene to the W_8 cubes occurs through the free OH group of one of the single-donor water molecules, the single-donor normal modes calculated for BW_8(cubic D_{2d}) and BW_8(cubic S_4) become partially localized, thereby redistributing the single-donor OH stretch intensity amongst the normal modes.

For both BW_8 isomers, the experimental spectra in the single-donor region have three resolved, approximately equally spaced transitions. The calculated spectrum of $BW_8(S_4)$ (Fig. 3C) reproduces both the spacing and the intensity profile of the experimental spectrum in this region (Fig. 3A). For $BW_8(D_{2d})$, the spacing between transitions is correct, but the relative intensities of the two highest frequency transitions is reversed (Fig. 3, B and D). This discrepancy may reflect a deficiency in the atomic basis sets.

The OH stretch IR spectra, especially in the double-donor region near 3550 cm^{-1}, provide unique spectral signatures of these cubic structures, distinguishing them from the bicoordinated cyclic structures of the water trimer to pentamer, and the tetracoordinated water molecules found in liquid water and ice.

It is hoped that the present data will stimulate further structural characterization of the D_{2d} and S_4 cubic structures of W_8. Despite their near identical rotational constants (Table 2), the rotational levels of the D_{2d} and S_4 structures will have different nuclear-spin statistical weights, which could be used in rotationally resolved spectra to distinguish the two structures. The cubic isomers may also differ in their hydrogen tunneling behavior.

REFERENCES AND NOTES

1. C. J. Tsai and K. D. Jordan, *J. Chem. Phys.* **95**, 3850 (1991).
2. C. Lee, H. Chen, G. Fitzgerald, *ibid.* **102**, 1266 (1995); R. Knochenmuss and S. Leutwyler, *ibid.* **96**, 5233 (1992); D. A. Estrin, L. Paglieri, G. Corongui, E. Clementi, *J. Phys. Chem.* **100**, 8701 (1996).
3. K. S. Kim, M. Dupuis, G. C. Lie, E. Clementi, *Chem. Phys. Lett.* **131**, 451 (1986); G. Brink and L. Glasser, *J. Phys. Chem.* **88**, 3412 (1984).
4. C. J. Tsai and K. D. Jordan, *J. Phys. Chem.* **97**, 5208 (1993).
5. D. J. Wales and I. Ohmine, *J. Chem. Phys.* **98**, 7245 (1993).
6. B. Rowland *et al.*, *ibid.* **102**, 8328 (1995).
7. Q. Du, R. Superfine, E. Freysz, Y. R. Shen, *Phys. Rev. Lett.* **70**, 2313 (1993).
8. G. C. Pimentel and A. L. McClellan, *The Hydrogen Bond* (Freeman, San Francisco, 1960).
9. F. Huisken, M. Kaloudis, A. Kulcke, *J. Chem. Phys.* **104**, 17 (1996), and references therein.
10. R. N. Pribble and T. S. Zwier, *Science* **265**, 75 (1994); *Discuss. Faraday Soc.* **97**, 229 (1994).
11. R. N. Pribble, A. W. Garrett, K. Haber, T. S. Zwier, *J. Chem. Phys.* **103**, 531 (1995).
12. S. Y. Fredericks, K. D. Jordan, T. S. Zwier, *J. Phys. Chem.* **100**, 7810 (1996).
13. T. S. Zwier, *Annu. Rev. Phys. Chem.* **47**, 205 (1996).
14. A. W. Garrett and T. S. Zwier, *J. Chem. Phys.* **96**, 3402 (1992).
15. A. J. Gotch and T. S. Zwier, *ibid.*, p. 3388.
16. A. E. W. Knight, C. S. Parmenter, M. W. Schuyler, *J. Am. Chem. Soc.* **97**, 1993 (1975).
17. R. N. Pribble, C. Gruenloh, T. S. Zwier, *Chem. Phys. Lett.* **262**, 627 (1996).
18. The Becke3LYP functional combines Becke's hybrid exchange functional [A. D. Becke, *J. Chem. Phys.* **98**, 5648 (1993)] and the LYP correlation functional [C. Lee, W. Yang, R. G. Parr, *Phys. Rev. B* **37**, 785 (1988)], with the weights of the various terms in the functional being the default values in Gaussian 94. The 6-31 +G[d,p] basis set combines the 6-31 +G basis set with the diffuse polarization functions from the aug-cc-pVDZ set [R. A. Kendall, T. H. Dunning Jr., R. J. Harrison, *J. Chem. Phys.* **96**, 6796 (1992)].
19. T. Clark, J. Chandrasekhar, G. W. Spitznagel, P. v. R Schleyer, *J. Comp. Chem.* **4**, 294 (1983); W. J. Hehre, R. Ditchfield, J. A. Pople, *J. Chem. Phys.* **56**, 2257 (1972); M. J. Frisch, J. A. Pople, J. S. Binkley, *ibid.* **80**, 3265 (1984).
20. K. Kim and K. D. Jordan, *J. Phys. Chem.* **98**, 10089 (1994).
21. Previous work (*12, 20, 22*) has demonstrated that DFT calculations using the Becke3LYP functional faithfully reproduce the trends in the OH stretch spectra of water and benzene-water clusters. The major deficiency of such calculations is an exaggeration of the magnitude of the shifts of the single-donor OH stretch frequencies.
22. J. E. Del Bene, W. B. Person, K. Szczepaniak, *J. Phys. Chem.* **99**, 10705 (1995); S. S. Xantheas, *J. Chem. Phys.* **102**, 4595 (1995).
23. Gaussian 94 (Rev. G); M. J. Frisch *et al.*, Gaussian Inc., Pittsburgh, PA (1995).
24. A table of the calculated vibrational frequencies, frequency shifts, and IR intensities for $W_8(D_{2d})$, $W_8(S_4)$, $BW_8(D_{2d})$, and $BW_8(S_4)$ is available on the World Wide Web at http://www.pitt.edu/~jordan/science_article/BW8/table
25. We gratefully acknowledge NSF for support of this research from grants CHE-9404716 and CHE-9422210. We thank C. Sosa of Silicon Graphics and Cray Research for assistance with some of the calculations.

7 February 1997; accepted 7 April 1997

Atomic Selectivity in the Chemisorption of ICl (Iodochloride) on Silicon Surfaces

Yong Liu, Denis P. Masson, Andrew C. Kummel*

When ICl adsorbs on a clean silicon (111)-(7×7) surface, the reaction is chemically selective. This process has been studied with the use of scanning tunneling microscopy and Auger spectroscopy. The dominant mechanism is the formation of silicon monoiodide by abstraction and the ejection of the chlorine atoms back into the gas phase. This pathway is not only chemically selective but also the least exothermic of all the possible reaction mechanisms. Although atomic chemical selectivity in gas-phase reactions is quite common, atomic chemical selectivity is unexpected in gas-surface reactions on clean surfaces because of the high density of reactive sites.

The gas-phase reaction of ICl molecules with deuterium is chemically selective; the yield of DI exceeds DCl by a factor of at least 3 despite the much lower exothermicity for forming DI (84 kJ mol^{-1}) compared with DCl (218 kJ mol^{-1}) (*1*). From a dynamical point of view, a fundamentally interesting question is whether such a chemical selectivity observed in gas-phase reactions can exist in molecule-surface interactions. For the chemisorption of ICl onto the Si(111)-(7×7) surface, there are three possible competitive reaction channels: dissociative adsorption (Eq. 1), chlorine-selective abstraction (Eq. 2), and iodine-selective abstraction (Eq. 3).

$$\text{I–Cl(g)} + 2\text{Si} \rightarrow \text{Si–I} + \text{Si–Cl}$$

$$\Delta E = -5.59\text{eV} \qquad (1)$$

$$\text{I–Cl(g)} + \text{Si} \rightarrow \text{Si–Cl} + \text{I(g)}$$

$$\Delta E = -2.55\text{eV} \qquad (2)$$

$$\text{I–Cl(g)} + \text{Si} \rightarrow \text{Si–I} + \text{Cl(g)}$$

$$\Delta E = -0.86\text{eV} \qquad (3)$$

In dissociative adsorption, the chemical bond of an ICl molecule breaks, so that the I and Cl atoms separately form chemical bonds with the surface. In abstractive adsorption, one halogen atom (X) in an ICl molecule forms a chemical bond with the surface and the other is ejected into the gas

---

Department of Chemistry, 0358, University of California at San Diego, 9500 Gilman Drive, La Jolla, CA 92093, USA.

*To whom correspondence should be addressed.